

Methods of Observing the Microwave Instability Above and Below Transition

E. Shaposhnikova, CERN, Geneva, Switzerland

Abstract

A short overview of different methods of observing the longitudinal microwave instability will be followed by a more detailed analysis of those based on beam spectra measurements. Results obtained in the CERN SPS, both above and below transition, will be presented together with data taken at other accelerators.

1 INTRODUCTION

A very wide range of phenomena in high intensity circular accelerators is called by the same name “microwave (μw) instability”. The instability known as turbulent bunch lengthening was observed already in the 70’s, first in electron accelerators and later in proton machines. Most probably, the name itself was first introduced by D. Boussard in 1975 [1] to describe an instability observed in the CERN PS during debunching of proton bunches and associated with microwave signals (frequencies above 1 GHz).

Later the name microwave instability was extended to coasting beams, in both transverse and longitudinal planes. Replacing average beam parameters by local ones the instability criteria derived for a coasting beam [2] was successfully applied to a bunched beam [1] confirming the similarity of the phenomena.

Usually, but not always, an instability is called the μw if

$$f_r \tau \gg 1, \quad (1)$$

where τ is the bunch length and $f_r = \omega_r/(2\pi)$ is the resonant impedance frequency. For a coasting beam this condition then means frequencies higher than the revolution frequency $f_0 = \omega_0/(2\pi)$ which can very well be in the kHz range. For very short electron bunches condition (1) can give $f_r > 100$ GHz. In this case the name μw is also used for instability driven by an impedance $Z(n)$, $n = f/f_0$, with a very high frequency f_r but which nevertheless doesn’t satisfy condition (1).

Below we will consider different methods of observing longitudinal single bunch instability together with information which can be obtained from the data. These methods are based on the phenomenological definition of the μw instability and can be grouped as measurements of

- increase of longitudinal emittance with intensity;
- high frequency beam spectrum.

2 EMITTANCE BLOW-UP

Increase of longitudinal emittance can be seen first of all as bunch lengthening. pushing bunch current to the limit

bunch lengthening is observed in practically all modern rings as well as in old accelerators.

Bunch lengthening due to μw instability can be distinguished from that connected with potential well distortion by a change in the slope of the curve giving bunch length as a function of intensity. This break point is considered as the instability threshold. Usually it corresponds to an intensity range ($10^{10} - 10^{11}$) particles per bunch.

Measurements of momentum spread $\Delta p/p$ allow μw instability to be distinguished from other intensity dependent effects (like, for example, intrabeam scattering) and define more precisely the threshold. In a bunched beam momentum spread can be found from an estimation of the transverse size in a dispersive region, from the debunching rate with RF off, and for electron bunches also from spectral analysis.

The threshold intensity substituted into the Keil-Schnell-Boussard criterion [1, 2] is often used to estimate the longitudinal impedance $|Z|/n$ of the ring. which varies from tens of Ohms in old accelerators to fractions of an Ohm in modern. Comparison of the slope of the bunch lengthening curve “before” and “after” gives a good indication about the global success of impedance reduction programmes (like in [3], [4]).

More information about the coupling impedance can be obtained from the dependence of bunch length on intensity above the threshold. Assuming that the emittance changes just enough to stay at the threshold, the frequency dependence of impedance can be estimated from the scaling law [5].

Most bunch lengthening curves are obtained above transition energy. Recent measurements of emittance blow-up of very short electron bunches [6, 7] with negative $\alpha = \gamma_t^{-2}$ (imaginary γ_t) are equivalent to measurements below transition, with negative slip factor $\eta = \alpha - \gamma^{-2}$. In Super-Aco [6], for the same $|\alpha| = 0.015$, bunch lengthening was stronger for $\alpha > 0$ and energy widening for $\alpha < 0$.

Except maybe for special behaviour of the bunch length such as the saw-tooth instability [3] or hysteresis [8]), in general measurements of unstable beam spectra can give more insight into the instability under study.

3 UNSTABLE BEAM SPECTRA

3.1 RF on

Let us first consider the situation where RF is on and synchrotron motion is important. If the frequency of the driving impedance is not high enough ($f_r \leq 1/\tau$), instability manifests itself as coherent synchrotron oscillations at low multipoles. In this case the stable bunch spectrum “sees”

the driving impedance and the effect of potential well distortion is important.

Measurements of the behaviour of synchrotron sidebands at $nf_0 + mf_s$ (spectrum analysis of pick-up signal with high resolution, if possible above the stable bunch spectrum, $nf_0 > 1/\tau$) can give interesting information about the mechanism of instability. Instability thresholds measured from momentum spread (SPEAR, TRISTAN-AR, LEP) coincide with an onset of coherent oscillations where one can see [9]:

- growing higher order azimuthal modes
- splitting of modes (radial modes?)

Unlike in the transverse plane, no clear azimuthal mode coupling has been observed in the longitudinal plane so far. Bunch spectrum functions [10] for radial modes (k) belonging to different azimuthal modes (m) can peak at the same frequency $\omega_{m,k}$ (for example for a Gaussian distribution $\omega_{m,k} = \sqrt{m + 2k}/\sigma_t$) and therefore are difficult to measure.

One can find some interesting features in the measurements done for short bunches in BESSY [11] and in the behaviour of azimuthal modes (jumping from sextupole to a quadrupole mode) discovered in SLC [12].

3.2 Transition crossing

In proton machines μw instability is often observed at transition crossing [4, 13, 14, 15]. In this special case the azimuthal motion in the phase space is practically frozen and particles are moving along momentum axes under the influence of external (RF) and induced voltages. It is noticed that strong microwave signals appear just above transition (AT) [4, 13, 15] which can be interpreted as a difference in bunch stability above and below transition (BT). In Fig. 1 one can clearly see the high frequency signal growing after transition crossing in the SPS [13]. With 2 ns long bunches signals were seen only above 1.2 GHz.

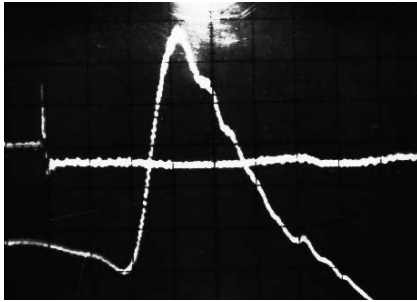


Figure 1: High frequency signal after transition crossing in the CERN SPS. Upper trace: RF phase with jump at transition, low trace: (2.6 - 3.2) GHz signal [13].

In a coasting beam a purely reactive impedance can cause negative mass instability for space charge AT and an inductive impedance BT. However it seems that strong μw signals were observed just after transition crossing in accelerators both with capacitive (space charge) [4] and in-

ductive type [13] of low frequency impedance, suggesting the possibility of another explanation. In fact in all cases in real accelerators measurements are unavoidably done in the presence of resistive impedances. Indeed "switching off" space charge in simulations does not change results [4] obtained for the resonant impedance

$$Z(\omega) = \frac{R_{sh}}{1 + iQ(\omega/\omega_r - \omega_r/\omega)}, \quad (2)$$

where R_{sh} is the shunt impedance, Q the quality factor.

Passing transition from the opposite side in simulations [15] also showed higher μw signal AT for resonant impedances. A suggested explanation [4, 15] is based on the fact that the tail of the bunch, mostly affected by the wake, sees a different type of external voltage in two cases (accelerating BT and decelerating AT).

3.3 RF off

Instability development is different if synchrotron motion is not important. For a proton beam μw signals are very often observed during RF gymnastics involving adiabatic reduction of RF voltage or a debunching process. The range of observed frequencies can give important information about possible source of instability [16, 17].

To analyse the linear stage of the instability one can use an expansion of the line density perturbation $\rho(\theta, t)$ in azimuthal harmonics: $\rho(\theta, t) = e^{-i\Omega t} \sum_n \rho_n e^{im\theta}$, where the unstable beam spectrum is given by ρ_n and the instability growth rate by $\text{Im}\Omega$. Since we assume being above the threshold of instability, a monoenergetic bunch with an initial distribution function $F(\theta, \dot{\theta}) = G(\theta)\delta(\dot{\theta})$ is considered.

Using the linearised Vlasov equation leads to the same matrix equation with RF on and off if the instability growth time $\text{Im}\Omega^{-1}$ is much less than synchrotron period $1/f_s$ or debunching time $t_d = \tau/(2|\eta|\frac{\Delta p}{p})$, see [17, 18],

$$\rho_n = -i \frac{\eta n \omega_0}{2\pi E_0} \left(\frac{e\omega_0}{\Omega}\right)^2 \sum_{n'} G_{n-n'} Z_{n'} \rho_{n'}, \quad (3)$$

where G_n is the Fourier transform of $G(\theta)$.

For a **coasting beam** $G_{n-n'} = N\delta_{n,n'}/(2\pi)$ and a growth rate can be found from the expression:

$$\Omega_n^2 = -i \left(\frac{en\omega_0}{2\pi}\right)^2 \frac{N\omega_0}{E_0} \eta \frac{Z_n}{n}. \quad (4)$$

For a reactive impedance, $Z = i\text{Im}Z$, this solution describes the negative mass instability which can occur if $\eta\text{Im}Z/n < 0$.

For a **single bunch** interacting with a resonant impedance (2), features of the spectrum can be obtained qualitatively under simplifying assumptions in two extreme cases: narrow-band, $\Delta\omega_r = \omega_r/2Q \ll 1/\tau$, and broad-band, $\Delta\omega_r\tau \gg 1$, impedances.

For **narrow-band impedance** the bunch spectrum in Eq. (3) can be assumed constant over the impedance width

with $G_{n-n'} \simeq G_{n-n_r}$ for $n' > 0$. Then

$$\frac{\text{Im}\Omega}{\omega_r} \simeq \left(\frac{Ne^2\omega_0|\eta|}{16\pi E_0} \frac{R_{sh}}{Q} \right)^{\frac{1}{2}}. \quad (5)$$

where N is the number of particles in the bunch.

The spectrum of the unstable modes is $\rho_n \sim nG_{n-n_r}$. It is centered at $n = n_r$ and has a width inversely proportional to the bunch length. The same spectrum is obtained with a narrow-band resistive impedance [19, 20].

By finding the maxima in the unstable spectrum it is possible to measure the frequency of the guilty impedance, see next Section. One can also hope to determine the R_{sh}/Q from Eq.(5) by measuring the growth rate of the unstable mode. However, in reality, due to the complicated structure of the signal in time the growth rate is often ill-defined.

For **broad-band impedance** approximation the bunch spectrum is replaced by a very narrow one. For a long Gaussian bunch ($\tau \simeq 4\sigma_t = 4\sigma/\omega_0$)

$$G_{n-n'} = \frac{N}{2\pi} \exp\left(-\frac{(n-n')^2\sigma^2}{2}\right) \approx \frac{N}{\sqrt{2\pi}\sigma} \delta_{n,n'}. \quad (6)$$

Then the expression for the instability growth rate is similar to a coasting beam where average current is replaced by peak, see also [19]:

$$\Omega_n^2 \simeq -i \frac{(en\omega_0)^2 N}{(2\pi)^{3/2} E_0 \sigma_t} \eta \frac{Z_n}{n}. \quad (7)$$

The bandwidth of the spectrum in this case is defined by the impedance bandwidth. In numerical simulations done by the author with ESME [21] it is also modulated with a wavelength close to the width of the stable bunch spectrum.

4 MEASUREMENTS IN THE CERN SPS

4.1 Experimental conditions and methods used

In the CERN SPS, $R = 1100$ m, $\gamma_t = 23.2$, μw instability was first observed below transition (10 GeV) during debunching of protons in 1977, almost from beginning of commissioning. Later, due to μw instability, single bunch intensity was limited at $N = 1.6 \times 10^{11}$ during $p\bar{p}$ collider operation (above transition), and at $N = 3.5 \times 10^{10}$ for leptons (3.5 GeV). Measurements of $|Z|/n$ made with different beams over the years give values in the range (10 - 40) Ohm.

Recent measurements of unstable bunch spectrum have allowed the sources of μw instability to be identified [17]. As a result in the SPS an extensive impedance reduction programme involving the work of a large team is close to completion.

Experiments were done with single bunches of similar intensity in the range ($5 \times 10^9 - 1 \times 10^{11}$) injected with RF off on an injection plateau at 14, 20 and 26 GeV. Bunches were sufficiently long, (20 - 50) ns and had small momentum spread (to be more unstable and debunch slowly).

Two methods of measurement and data analysis were used:

(I) Measurement of maximum signal at a given frequency directly from a spectrum analyzer connected to a wideband pick-up, PU, (4 MHz - 4 GHz).

(II) Measurement of bunch profile (signal from the same PU) each X turns followed by Fourier analysis. This approach was restricted to a maximum frequency of 2 GHz due to the 4 GHz sampling rate of the digital oscilloscope.

Recording the maximum mode amplitude of the signal reached during the observation time 50 ms (less than t_d) at different frequencies, method (I), and using statistics (data from > 10 bunches with similar intensity) led to the global spectral distribution presented in Fig. 2. Similar results were obtained below 2 GHz using method (II). Various peaks correspond to different impedances in the ring, with bandwidth $\Delta\omega_r$ both larger and smaller than $1/\tau \sim 40$ MHz.

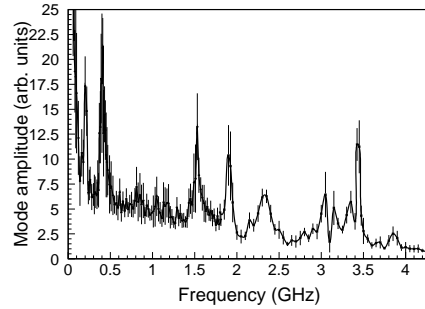


Figure 2: Spectral distribution measured with $\tau = 25$ ns and emittance $\varepsilon = 0.24$ eVs, 1996.

4.2 Results above and below transition

Future CERN projects - LHC and CNGS, require higher single bunch intensities injected into the SPS both above (26 GeV) and below (14 GeV) transition energy.

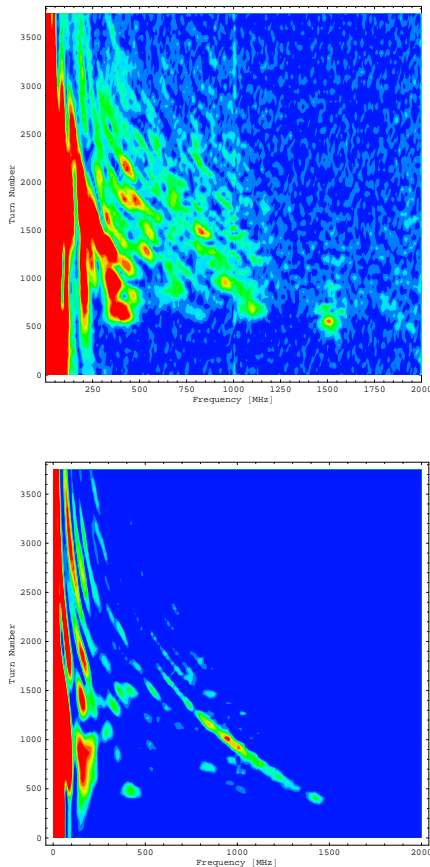
First measurements below transition (BT) using the method described above were made in 1996 at 14 GeV (see Fig. 4, left). They basically showed the same peaks as in Fig. 2 however smeared out by fast debunching due to the large value of η . Later the injection energy was specially adjusted in studies to have parameters comparable with ones in measurements already done above transition (AT). Relevant beam and machine parameters from the last experiment [23] are presented in Table 1. In both cases the bunch intensity was $N = 3.5 \times 10^{10}$. In all the measurements described here $\gamma_t = 23.2$. Measurements done for the same bunches and two different transition energies are presented in [24]. As expected they have demonstrated much better bunch stability at low $\gamma_t = 19.6$.

Single bunches with similar parameters are unstable both below and above transition. Contrary to what one would expect from potential well distortion (defocusing AT and focusing BT for inductive type of low frequency impedance

E	GeV	20	26
τ	ns	22	24
$\Delta p/p$		$\pm 2.9 \times 10^{-4}$	$\pm 2.5 \times 10^{-4}$
η		-3.46×10^{-4}	5.53×10^{-4}
t_d	ms	110	87

Table 1: Beam and machine parameters

in the SPS), faster debunching was observed BT. This observation can be explained by the fact that the tail of the bunch is affected first by the wake. Particles lose energy creating a microstructure which has significantly lower energy BT due to the opposite directions of bunch rotation in phase space AT and BT. As a result BT total momentum blow-up is larger and debunching is faster. This is true even for exactly the same $|\eta|$ used in simulations [23] done with ESME. Fast debunching stretches microbunches and leads to the frequency sweep well seen in Fig. 3, method (II).


 Figure 3: Contour plot in frequency domain at 26 GeV (top) and 20 GeV (bottom), $N = 3.4 \times 10^{10}$.

Bunch spectra showing resonant structure agree very well both BT and AT if for the measurements BT only results at the beginning of debunching are taken into account. Excitation of high frequencies is dominant BT and almost suppresses other peaks with lower frequency, which are well seen AT. It is also interesting that, when sweep-

ing through lower frequencies, the amplitude of excitation created initially at 1.5 GHz grows when passing the frequencies of other impedances both known (800 MHz) and under suspicion (e.g around 1 GHz).

For frequencies above 2 GHz measurements were done using method (I). The data for the two energies BT - 14 GeV and 20 GeV, shown in Fig. 4, have the same resonant structure as AT, see Fig. 2.

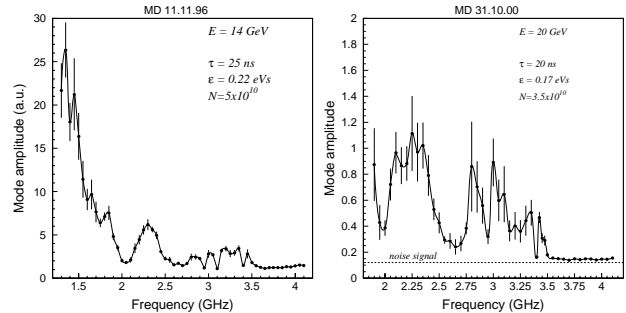


Figure 4: Mode amplitude measured below transition at 14 GeV (left) and 20 GeV (right).

4.3 Search for impedances continues...

Most of the peaks seen in Fig. 2 were identified with different resonant impedances in the ring (mainly fundamental and HOMs of RF cavities and intermagnet vacuum ports). However the source of impedance at 400 MHz was not obvious. High signal amplitude suggested a significant impedance, comparable with the impedance of the 200 MHz TW RF system ($R_{sh}/Q \sim 23$ kOhm, $Q \sim 130$) also seen well in Fig. 2.

Simple estimations show that a cavity-like object with radius around 30 cm is required to have lowest resonant frequency at 400 MHz. The list of different types of objects found in the ring at that time contained 15 items. Among them were the 400 MHz LHC prototype cavity (removed from the ring at the beginning of 1999), electrostatic septa (10 tanks), injection and extraction proton kickers MKE and MKP (14 modules), extraction septa (16 tanks) and equipment for injection and extraction of leptons, (removed from the ring during 2000/2001 shutdown).

Extraction septa, which were seriously suspected due to their large number, were shielded during the 1999/2000 shutdown. Beam measurements done in 2000 showed that in spite of this shielding the instability is still there.

The signal at 400 MHz will be always produced as a high harmonic of the mode excited by the 200 MHz RF system due to the nonlinearity of the process, but its amplitude can not exceed a half of the main, 200 MHz harmonic. To see the effect of shielding relative measurements of the maximum amplitude at 200 MHz, A_{200} and 400 MHz, A_{400} , as a function of intensity were made. In Fig. 5 reference measurements of A_{200} and A_{400} from 1999, before shielding the septa, are presented together with data from 2000.

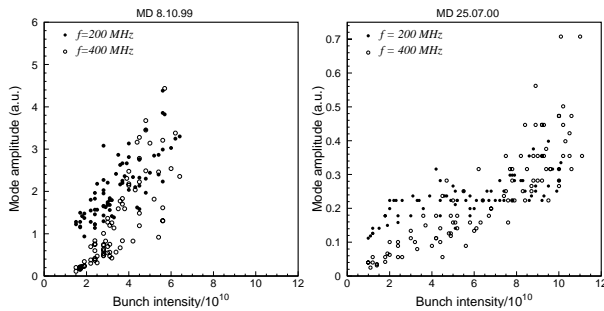


Figure 5: Mode amplitude at 200 MHz and 400 MHz as a function of bunch intensity measured at 26 GeV in 1999 ($\tau = 26$ ns, $\varepsilon = 0.24$ eVs) and 2000 ($\tau = 21$ ns, $\varepsilon = 0.24$ eVs).

One can see that the 400 MHz threshold (bunch intensity at which $A_{400} \sim A_{200}$) increased in 2000. This can be interpreted as the result of shielding the septa. However more detailed studies showed that this increase can be attributed, at least partially, to the slightly different bunch lengths used in measurements.

Measurements of A_{200} and A_{400} as a function of bunch length for constant emittance and intensity are shown in Fig. 6. Indeed the ratio A_{400}/A_{200} decreases with decreasing bunch length. Similar measurements were also done at 20 GeV, Fig. 6 (right). There the variation of A_{400} with bunch length is less pronounced.

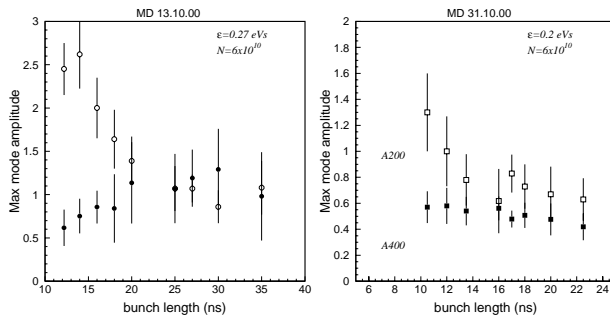


Figure 6: Mode amplitude at 200 MHz (empty symbols) and 400 MHz (filled symbols) measured at 26 GeV (left) and 20 GeV (right) as a function of bunch length for constant emittance and intensity (6×10^{10}).

Recent bench measurements of the MKE kicker tank with a single module showed significant impedance at 400 MHz, $R_{sh} \simeq 6$ kOhm. This is considered at the moment the best candidate for 400 MHz instability. Whether it is true will be known in 2003 after shielding of all tanks.

5 SUMMARY

Microwave instability can be identified from observation of intensity dependent emittance blow-up associated with growth of high frequency signals. In many cases the source of instability is a high frequency resonant impedance with

bandwidth larger or smaller than the width of stable bunch spectrum $\propto 1/\tau$. For relatively short bunches instability is seen as coherent oscillations at multiples of the synchrotron frequency. There is no clear experimental evidence for azimuthal mode coupling.

In the presence of resistive impedance the instability is observed both below and above transition, with RF on and off. For comparison of the thresholds more studies are necessary.

With RF on emittance blow-up was measured for negative α , equivalent to being below transition.

Under certain conditions measurements with RF off allow the sources of microwave instability to be seen, both below and above transition, and the impedance reduction programme to be followed up in detail.

The author is grateful to T. Bohl and T. Linnecar for useful discussions and helpful collaboration.

6 REFERENCES

- [1] D. Boussard, CERN Report LabII/RF/Int./75-2, 1975.
- [2] V.K. Neil, A.M. Sessler, Rev. Sci. Instr. **6**, 429 (1965); E. Keil, W. Schnell, CERN Report ISR-TH-RF/69-48, 1969.
- [3] K. Bane et al., PAC'95, 3109 (1995).
- [4] K. Takayama et al., Phys. Rev. Lett., **78**, 871 (1997); KEK Preprint 97-81, 1997.
- [5] A.W. Chao, J. Gareyte, Part. Acc. **25**, 229 (1990).
- [6] R.J. Bakker et al., EPAC'96, 667 (1996).
- [7] C. Limbourg, EPAC'98, 151 (1998).
- [8] T. Ieiri, EPAC'96, 1066 (1996).
- [9] P.B. Wilson et al., IEEE NS-24, 1211 (1977); K. Satoh, in KEK Report 90-21 (1991); D. Brandt, K. Cornelis, A. Hofmann, EPAC'92, 345 (1992).
- [10] F.J. Sacherer, IEEE NS-24, 1393 (1977).
- [11] W. Anders, BESSY Storage Ring, 3rd EPAC, 798 (1992).
- [12] B. Podobedov, R. Siemann, PAC'99, 146 (1999).
- [13] D. Boussard et al., IEEE, NS-26, No. 3, 3484 (1979).
- [14] K.-Y. Ng, FNAL-TM-1383, 1986.
- [15] V.I. Balbekov, A.Yu. Malovitsky, IHEP Preprint 86-74, Serpukhov, 1986.
- [16] V.I. Balbekov et al., IHEP Preprint 85-129, Serpukhov, 1985.
- [17] T. Bohl, T.P.R. Linnecar, E. Shaposhnikova, Phys. Rev. Lett., **78**, 3109 (1997).
- [18] J.M. Wang, C. Pellegrini, Proc. 11th Int. Conf. High Energy Acc., 554 (1980).
- [19] S. Krinsky, J.M. Wang, IEEE NS-30, 2494 (1983).
- [20] K.-Y. Ng, Proc. Sum. Study on Phys. of SSC, 590 (1986).
- [21] J. MacLachlan, Fermilab Report No. TM-1716, 1991.
- [22] D. Boussard et al., IEEE, NS-24, No.3, 1399 (1977).
- [23] T. Bohl, T. Linnecar, E. Shaposhnikova, EPAC 2000, p.1173; CERN SL-Note-2000-046 MD (2000).
- [24] T. Bohl et al., EPAC'98, 975 (1998).